

**Technical Justification for  
Eliminating Large Primary Loop  
Pipe Rupture as the Structural  
Design Basis for the R. E. Ginna  
Nuclear Power Plant for the  
License Renewal Program**

WCAP-15837 – NP Revision 0

**Technical Justification for Eliminating Large Primary Loop  
Pipe Rupture as the Structural Design Basis for the R. E.  
Ginna Nuclear Power Plant for the License Renewal Program**

**D. C. Bhowmick  
C. K. Ng**

**May 2003**

Verifier: *J. F. Petsche*  
J. F. Petsche

Approved: *S. A. Swamy*  
S. A. Swamy, Manager  
Structural Mechanics Technology

---

Westinghouse Electric Company LLC  
P.O. Box 355  
Pittsburgh, PA 15230-0355  
©2003 Westinghouse Electric Company LLC  
All rights Reserved

---

---

**TABLE OF CONTENTS**

<b>EXECUTIVE SUMMARY .....</b>	<b>vii</b>
<b>1.0 Introduction .....</b>	<b>1-1</b>
1.1 Purpose .....	1-1
1.2 Background Information .....	1-1
1.3 Scope and Objectives .....	1-2
1.4 References .....	1-3
<b>2.0 OPERATION AND STABILITY OF THE REACTOR COOLANT SYSTEM.....</b>	<b>2-1</b>
2.1 Stress Corrosion Cracking .....	2-1
2.2 Water Hammer.....	2-2
2.3 Low Cycle and High Cycle Fatigue.....	2-3
2.4 References .....	2-3
<b>3.0 PIPE GEOMETRY AND LOADING .....</b>	<b>3-1</b>
3.1 Introduction to Methodology .....	3-1
3.2 Calculation of Loads and Stresses .....	3-1
3.3 Loads for Leak Rate Evaluation .....	3-2
3.4 Load Combination for Crack Stability Analyses .....	3-3
3.5 References .....	3-3
<b>4.0 MATERIAL CHARACTERIZATION.....</b>	<b>4-1</b>
4.1 Primary Loop Pipe and Fittings Materials .....	4-1
4.2 Tensile Properties .....	4-1
4.3 Fracture Toughness Properties .....	4-2

---

4.4	References .....	4-5
5.0	CRITICAL LOCATIONS AND EVALUATION CRITERIA.....	5-1
5.1	Critical Locations.....	5-1
5.2	Fracture Criteria.....	5-1
6.0	LEAK RATE PREDICTIONS .....	6-1
6.1	Introduction .....	6-1
6.2	General Considerations .....	6-1
6.3	Calculation Method .....	6-1
6.4	Leak Rate Calculations .....	6-2
6.5	References .....	6-2
7.0	FRACTURE MECHANICS EVALUATION .....	7-1
7.1	Local Failure Mechanism .....	7-1
7.2	Global Failure Mechanism.....	7-1
7.3	Results of Crack Stability Evaluation.....	7-3
7.4	References .....	7-5
8.0	FATIGUE CRACK GROWTH ANALYSIS .....	8-1
8.1	References .....	8-2
9.0	ASSESSMENT OF MARGINS .....	9-1
10.0	CONCLUSIONS .....	10-1
	APPENDIX A.....	A-1
	LIMIT MOMENT .....	A-1

---

**LIST OF TABLES**

Table 3-1	Dimensions, Normal Loads and Normal Stresses for Ginna Station.....	3-4
Table 3-2	Faulted Loads and Stresses for Ginna Station .....	3-5
Table 4-1	Measured Tensile Properties (psi) for the Ginna Station Primary Loop Piping (Material A376 TP316).....	4-6
Table 4-2	Measured Tensile Properties (psi) for the Ginna Station Primary Loop Elbow Fittings (Material A351 CF8M) .....	4-7
Table 4-3	Mechanical Properties for Ginna Station Materials at Operating Temperatures	4-8
Table 4-4	Chemistry and Fracture Toughness Properties of the Material Heats of Ginna Station.....	4-9
Table 4-5	Fracture Toughness Properties for Ginna Station Primary Loops for Leak-Before-Break Evaluation at Critical Locations.....	4-10
Table 6-1	Flaw Sizes Yielding a Leak Rate of 2.5 gpm at the Governing Locations.....	6-3
Table 7-1	Stability Results for Ginna Station Based on Elastic J-Integral Evaluations.....	7-6
Table 7-2	Stability Results for Ginna Station Based on Limit Load .....	7-6
Table 8-1	Summary of Reactor Vessel Transients (60 Years).....	8-3
Table 8-2	Fatigue Crack Growth at [ $J^{a,c,e}$ ( 60 years).....	8-4
Table 9-1	Leakage Flaw Sizes, Critical Flaw Sizes and Margins for Ginna Station .....	9-2

---

**LIST OF FIGURES**

Figure 3-1	Hot Leg Coolant Pipe.....	3-6
Figure 3-2	Schematic Diagram of Ginna Station Primary Loop Showing Weld Locations..	3-7
Figure 4-1	Pre-Service J vs. $\Delta a$ for SA351 CF8M Cast Stainless Steel at 600°F .....	4-13
Figure 6-1	Analytical Predictions of Critical Rates of Steam-Water Mixtures .....	6-4
Figure 6-2	[ $J^{a,c,e}$ Pressure Ratio as a Function of L/D .....	6-5
Figure 6-3	Idealized Pressure Drop Profile Through a Postulated Crack.....	6-6
Figure 7-1	[ $J^{a,c,e}$ Stress Distribution .....	7-7
Figure 7-2	Critical Flaw Size Prediction – Hot Leg at Location 1 .....	7-8
Figure 7-3	Critical Flaw Size Prediction – Hot Leg at Location 3 .....	7-9
Figure 7-4	Critical Flaw Size Prediction – Cold Leg at Location 12.....	7-10
Figure 8-1	Typical Cross-Section of [ $J^{a,c,e}$ .....	8-5
Figure 8-2	Reference Fatigue Crack Growth Curves for Carbon and Low Alloy Ferritic Steels .....	8-6
Figure A-1	Pipe with a Through-Wall Crack in Bending .....	A-2

## EXECUTIVE SUMMARY

The original structural design basis of the Reactor Coolant System (RCS) for the Rochester Gas and Electric Corporation Ginna Nuclear Power Plant required consideration of dynamic effects resulting from pipe break and that protective measures for such breaks be incorporated into the design. Subsequent to the original Ginna design, additional concern of asymmetric blowdown loads was raised as described in Unresolved Safety Issue A-2 (Asymmetric Blowdown Loads on the Reactor Coolant System) and Generic Letter 84-04 (Reference 1-2). However, research by the Nuclear Regulatory Commission (NRC) and industry coupled with operating experience determined that safety could be negatively impacted by placement of pipe whip restraints on certain systems. As a result, NRC and industry initiatives resulted in demonstrating that Leak-Before-Break (LBB) criteria can be applied to Reactor Coolant System piping based on fracture mechanics technology and material toughness. Generic analyses by Westinghouse for the application of LBB for specific plants were documented in response to the Unresolved Safety Issue A-2 in the NRC letter dated May 6, 1986 (Reference 1-3).

This present WCAP report documents the plant specific geometry, loading, and material properties used in the fracture mechanics evaluation. It also includes the temperature, pressure and loadings generated as a result of the Ginna Nuclear Power Plant License Renewal Program. Mechanical properties were determined at operating temperatures. Since the piping system includes cast stainless steel fittings, the end of life (60 year) fracture toughness considering thermal aging was determined for each heat of material.

Based on loading, pipe geometry and fracture toughness considerations, enveloping critical locations were determined at which Leak-Before-Break crack stability evaluations were made. Through-wall flaw sizes were postulated which would cause a leak at a rate of ten times the leakage detection system capability of the plant. Large margins for such flaw sizes were demonstrated against flaw instability. Finally, using thermal transient stresses and cycles, fatigue crack growth for 60 years was shown to be acceptable for the primary loops. All the recommended LBB margins (margin on leak rate, margin on flaw size and margin on loads) are satisfied.

It is therefore concluded that the dynamic effects of RCS primary loop pipe breaks need not be considered in the structural design basis of the Ginna Nuclear Power Plant for the License Renewal Program.

## 1.0 INTRODUCTION

### 1.1 PURPOSE

This report applies to the Ginna Station Reactor Coolant System (RCS) primary loop piping. It is intended to demonstrate that for the specific parameters of the Ginna Station, RCS primary loop pipe breaks need not be considered in the structural design basis for the 60 year plant life. The Nuclear Regulatory Commission (NRC) (Reference 1-2) has accepted the approach taken.

### 1.2 BACKGROUND INFORMATION

Westinghouse has performed considerable testing and analysis to demonstrate that RCS primary loop pipe breaks can be eliminated from the structural design basis of all Westinghouse plants. The concept of eliminating pipe breaks in the RCS primary loop was first presented to the NRC in 1978 in WCAP-9283 (Reference 1-4). That topical report employed a deterministic fracture mechanics evaluation and a probabilistic analysis to support the elimination of RCS primary loop pipe breaks from the structural design basis. That approach was then used as a means of addressing Generic Issue A-2 and Asymmetric LOCA Loads.

Westinghouse performed additional testing and analysis to justify the elimination of RCS primary loop pipe breaks from the structural design basis. This material was provided to the NRC along with Letter Report NS-EPR-2519 (Reference 1-5).

The NRC funded research through Lawrence Livermore National Laboratory (LLNL) to address this same issue using a probabilistic approach. As part of the LLNL research effort, Westinghouse performed extensive evaluations of specific plant loads, material properties, transients, and system geometries to demonstrate that the analysis and testing previously performed by Westinghouse and the research performed by LLNL applied to all Westinghouse plants (References 1-6 and 1-7). The results from the LLNL study were released at a March 28, 1983, ACRS Subcommittee meeting. These studies, which are applicable to all Westinghouse plants east of the Rocky Mountains, determined the mean probability of a direct LOCA (RCS primary loop pipe break) to be  $4.4 \times 10^{-12}$  per reactor year and the mean probability of an indirect LOCA to be  $10^{-7}$  per reactor year. Thus, the results previously obtained by Westinghouse (Reference 1-4) were confirmed by an independent NRC research study.

Based on the studies by Westinghouse, LLNL, the ACRS, and the AIF, NRC completed a safety review of the Westinghouse reports submitted to address asymmetric blowdown loads that result from a number of discrete break locations on the Pressurized Water Reactor (PWR) primary systems. The NRC Staff evaluation (Reference 1-2) concludes that an acceptable technical basis has been provided so that asymmetric blowdown loads need not be considered for those plants that can demonstrate the applicability of the modeling and conclusions contained in the Westinghouse response or can provide an equivalent fracture mechanics demonstration of the primary coolant loop integrity. In a more formal recognition of Leak-Before-Break (LBB) methodology applicability for PWRs, the NRC appropriately modified

10CFR 50, General Design Criterion 4, "Requirements for Protection Against Dynamic Effects for Postulated Pipe Rupture" (Reference 1-8).

### **1.3 SCOPE AND OBJECTIVES**

The general purpose of this investigation is to demonstrate Leak-Before-Break for the primary loops in the Ginna Station on a plant specific basis for the 60 year plant life. The recommendations and criteria proposed in Reference 1-9 are used in this evaluation. These criteria and resulting steps of the evaluation procedure can be briefly summarized as follows:

1. Calculate the applied loads. Identify the locations at which the highest faulted stress occurs.
2. Identify the materials and the associated material properties.
3. Postulate a surface flaw. Determine fatigue crack growth. Show that a through-wall crack will not result.
4. Postulate a through-wall flaw at the governing location(s). The size of the flaw should be large enough so that the leakage is assured of detection with margin using the installed leak detection equipment when the pipe is subjected to normal operating loads. A margin of 10 is demonstrated between the calculated leak rate and the leak detection capability.
5. Using faulted loads, demonstrate that there is a margin of 2 between the leakage flaw size and the critical flaw size.
6. Review the operating history to ascertain that operating experience has indicated no particular susceptibility to failure from the effects of corrosion, water hammer or low and high cycle fatigue.
7. For the materials actually used in the plant, provide the properties including toughness and tensile test data. Evaluate long term effects such as thermal aging.
8. Demonstrate margin on applied load.

This report provides a fracture mechanics demonstration of primary loop integrity for the Ginna Station which is consistent with the NRC position for exemption from consideration of dynamic effects.

The computer codes that are used in this evaluation for leak rate and fracture mechanics calculations have been validated and used for all the LBB applications by Westinghouse.

---

## 1.4 REFERENCES

- 1-1 WCAP-7211, Revision 4, "Energy Systems Business Unit Policy and Procedures for Management, Classification, and Release of Information," January 2001.
- 1-2 USNRC Generic Letter 84-04, Subject "Safety Evaluation of Westinghouse Topical Reports Dealing with Elimination of Postulated Pipe Breaks in PWR Primary Main Loops," February 1, 1984.
- 1-3 Nuclear Regulatory Commission Docket #'s 50-266 and 50-301 Letter from G. E. Lear, Director PWR Project Directorate #1 Division of PWR Licensing-A, NRC, to C. W. Fay, Vice President Nuclear Power Department Wisconsin Electric Power Company.
- 1-4 WCAP-9283, "The Integrity of Primary Piping Systems of Westinghouse Nuclear Power Plants During Postulated Seismic Events," March 1978.
- 1-5 Letter Report NS-EPR-2519, Westinghouse (E. P. Rahe) to NRC (D. G. Eisenhower), Westinghouse Proprietary Class 2, and November 10, 1981.
- 1-6 Letter from Westinghouse (E. P. Rahe) to NRC (W. V. Johnston) dated April 25, 1983.
- 1-7 Letter from Westinghouse (E. P. Rahe) to NRC (W. V. Johnston) dated July 25, 1983.
- 1-8 Nuclear Regulatory Commission, 10 CFR 50, Modification of General Design Criteria 4 Requirements for Protection Against Dynamic Effects of Postulated Pipe Ruptures, Final Rule, Federal Register/Vol. 52, No. 207/Tuesday, October 27, 1987/Rules and Regulations, pp. 41288-41295.
- 1-9 Standard Review Plan: Public Comments Solicited; 3.6.3 Leak-Before-Break Evaluation Procedures; Federal Register/Vol. 52, No. 167/Friday August 28, 1987/Notices, pp. 32626-32633.

## **2.0 OPERATION AND STABILITY OF THE REACTOR COOLANT SYSTEM**

### **2.1 STRESS CORROSION CRACKING**

The Westinghouse RCS primary loops have an operating history that demonstrates the inherent operating stability characteristics of the design. This includes a low susceptibility to cracking failure from the effects of corrosion (e.g., intergranular stress corrosion cracking (IGSCC)). This operating history totals over 1100 reactor-years, including 5 plants each having over 30 years of operation, 4 plants each with over 25 years of operation, 12 plants each with over 20 years of operation and 8 plants each with over 15 years of operation.

In 1978, the United States Nuclear Regulatory Commission (USNRC) formed the second Pipe Crack Study Group. (The first Pipe Crack Study Group (PCSG) established in 1975 addressed cracking in boiling water reactors only.) One of the objectives of the second PCSG was to include a review of the potential for stress corrosion cracking in Pressurized Water Reactors (PWR's). The results of the study performed by the PCSG were presented in NUREG-0531 (Reference 2-1) entitled "Investigation and Evaluation of Stress-Corrosion Cracking in Piping of Light Water Reactor Plants." In that report the PCSG stated:

"The PCSG has determined that the potential for stress-corrosion cracking in PWR primary system piping is extremely low because the ingredients that produce IGSCC are not all present. The use of hydrazine additives and a hydrogen overpressure limit the oxygen in the coolant to very low levels. Other impurities that might cause stress-corrosion cracking, such as halides or caustic, are also rigidly controlled. Only for brief periods during reactor shutdown when the coolant is exposed to the air and during the subsequent startup are conditions even marginally capable of producing stress-corrosion cracking in the primary systems of PWRs. Operating experience in PWRs supports this determination. To date, no stress corrosion cracking has been reported in the primary piping or safe ends of any PWR."

During 1979, several instances of cracking in PWR feedwater piping led to the establishment of the third PCSG. The investigations of the PCSG reported in NUREG-0691 (Reference 2-2) further confirmed that no occurrences of IGSCC have been reported for PWR primary coolant systems.

As a result of the recent issue of Primary Water Stress Corrosion Cracking (PWSCC) occurring in V. C. Summer reactor vessel hot leg nozzle, Alloy 82/182 weld is being currently investigated under the EPRI Material Reliability Project (MRP) Program. It should be noted that the susceptible material under investigation is not found in the primary loop piping at the Ginna Station.

For stress corrosion cracking (SCC) to occur in piping, the following three conditions must exist simultaneously: high tensile stresses, susceptible material, and a corrosive environment. Since some residual stresses and some degree of material susceptibility exist in any stainless steel

pipng, the potential for stress corrosion is minimized by properly selecting a material immune to SCC as well as preventing the occurrence of a corrosive environment. The material specifications consider compatibility with the system's operating environment (both internal and external) as well as other material in the system, applicable ASME Code rules, fracture toughness, welding, fabrication, and processing.

The elements of a water environment known to increase the susceptibility of austenitic stainless steel to stress corrosion are: oxygen, fluorides, chlorides, hydroxides, hydrogen peroxide, and reduced forms of sulfur (e.g., sulfides, sulfites, and thionates). Strict pipe cleaning standards prior to operation and careful control of water chemistry during plant operation are used to prevent the occurrence of a corrosive environment. Prior to being put into service, the piping is cleaned internally and externally. During flushes and preoperational testing, water chemistry is controlled in accordance with written specifications. Requirements on chlorides, fluorides, conductivity, and pH are included in the acceptance criteria for the piping.

During plant operation, the reactor coolant water chemistry is monitored and maintained within very specific limits. Contaminant concentrations are kept below the thresholds known to be conducive to stress corrosion cracking with the major water chemistry control standards being included in the plant operating procedures as a condition for plant operation. For example, during normal power operation, oxygen concentration in the RCS is expected to be in the ppb range by controlling charging flow chemistry and maintaining hydrogen in the reactor coolant at specified concentrations. Halogen concentrations are also stringently controlled by maintaining concentrations of chlorides and fluorides within the specified limits. Thus during plant operation, the likelihood of stress corrosion cracking is minimized.

## **2.2 WATER HAMMER**

Overall, there is a low potential for water hammer in the RCS since it is designed and operated to preclude the voiding condition in normally filled lines. The reactor coolant system, including piping and primary components, is designed for normal, upset, emergency, and faulted condition transients. The design requirements are conservative relative to both the number of transients and their severity. Relief valve actuation and the associated hydraulic transients following valve opening are considered in the system design. Other valve and pump actuations are relatively slow transients with no significant effect on the system dynamic loads. To ensure dynamic system stability, reactor coolant parameters are stringently controlled. Temperature during normal operation is maintained within a narrow range; pressure is controlled by pressurizer heaters and pressurizer spray also within a narrow range for steady-state conditions. The flow characteristics of the system remain constant during a fuel cycle because the only governing parameters, namely system resistance and the reactor coolant pump characteristics, are controlled in the design process. Additionally, Westinghouse has instrumented typical reactor coolant systems to verify the flow and vibration characteristics of the system. Preoperational testing and operating experience has verified the Westinghouse approach. The operating transients of the RCS primary piping are such that no significant water hammer can occur.

---

## 2.3 LOW CYCLE AND HIGH CYCLE FATIGUE

An assessment of the low cycle fatigue loadings was carried out as part of this study in the form of a fatigue crack growth analysis, as discussed in Section 8.0.

High cycle fatigue loads in the system would result primarily from pump vibrations. These are minimized by restrictions placed on shaft vibrations during hot functional testing and operation. During operation, an alarm signals the exceedence of the vibration limits. Field measurements have been made on a number of plants during hot functional testing, including plants similar to the Ginna Station. Stresses in the elbow below the reactor coolant pump resulting from system vibration have been found to be very small, between 2 and 3 ksi at the highest. These stresses are well below the fatigue endurance limit for the material and would also result in an applied stress intensity factor below the threshold for fatigue crack growth.

## 2.4 REFERENCES

- 2-1 Investigation and Evaluation of Stress-Corrosion Cracking in Piping of Light Water Reactor Plants, NUREG-0531, U.S. Nuclear Regulatory Commission, February 1979.
- 2-2 Investigation and Evaluation of Cracking Incidents in Piping in Pressurized Water Reactors, NUREG-0691, U.S. Nuclear Regulatory Commission, September 1980.

## 3.0 PIPE GEOMETRY AND LOADING

### 3.1 INTRODUCTION TO METHODOLOGY

The general approach is discussed first. As an example, a segment of the primary coolant hot leg pipe is shown in Figure 3-1. The outside diameter and minimum wall thickness of the pipe are 33.875 in. and 2.333 in., respectively, as shown in the figure. The normal stresses at the weld locations are from the load combination procedure discussed in Section 3.3 whereas the faulted loads are as described in Section 3.4. The components for normal loads are pressure, deadweight and thermal expansion. An additional component, Safe Shutdown Earthquake (SSE), is considered for faulted loads. As seen from Table 3-2, the highest stressed location in the entire loop is at Location 1 at the reactor vessel outlet nozzle to pipe weld. This highest stressed location is a load critical location and is one of the locations at which, as an enveloping location, Leak-Before-Break is to be established. Essentially, a circumferential flaw postulated to exist at this location is subjected to both the normal loads and faulted loads to assess leakage and stability, respectively. The loads at this location are also given in Figure 3-1.

Since the elbows are made of cast stainless steel, thermal aging must be considered (Section 4.0). Thermal aging results in lower fracture toughness. Thus, locations other than the load critical locations must be examined by taking into consideration both fracture toughness and stress. The enveloping locations so determined are called toughness critical locations. Once loads (Section 3.0) and fracture toughness (Section 4.0) are obtained, the load critical and toughness critical locations are determined (Section 5.0). At these locations, leak rate evaluations (Section 6.0) and fracture mechanics evaluations (Section 7.0) are performed per the guidance of Reference 3-1. Fatigue crack growth (Section 8.0) and stability margins are also evaluated (Section 9.0).

The weld locations being evaluated are shown in Figure 3-2.

### 3.2 CALCULATION OF LOADS AND STRESSES

The stresses due to axial loads and moments are calculated by the following equation:

$$\sigma = \frac{F}{A} + \frac{M}{Z} \quad (3-1)$$

where,

$\sigma$  = Stress  
 $F$  = Axial Load

M	=	Moment
A	=	Pipe Cross-Sectional Area
Z	=	Section Modulus

The moments for the desired loading combinations are calculated by the following equation:

$$M = (M_x^2 + M_y^2 + M_z^2)^{1/2} \quad (3-2)$$

where,

M	=	Moment for Required Loading
M <sub>x</sub>	=	X Component of Bending Moment
M <sub>y</sub>	=	Y Component of Bending Moment
M <sub>z</sub>	=	Z Component of Bending Moment

NOTE: X-axis is along the centerline of the pipe.

The axial load and moments for leak rate predictions and crack stability analyses are computed by the methods to be explained in Sections 3.3 and 3.4.

### 3.3 LOADS FOR LEAK RATE EVALUATION

The normal operating loads for leak rate predictions are calculated by the following equations:

$$F = F_{DW} + F_{TH} + F_P \quad (3-3)$$

$$M_x = (M_x)_{DW} + (M_x)_{TH} \quad (3-4)$$

$$M_y = (M_y)_{DW} + (M_y)_{TH} \quad (3-5)$$

$$M_z = (M_z)_{DW} + (M_z)_{TH} \quad (3-6)$$

The subscripts of the above equations represent the following loading cases:

DW	=	Deadweight
TH	=	Normal Thermal Expansion
P	=	Load Due To Internal Pressure

This method of combining loads is often referred as the algebraic sum method (Reference 3-1).

The loads based on this method of combination are provided in Table 3-1 at all the weld locations identified in Figure 3-2. The outside diameter and minimum thickness are also given.

### 3.4 LOAD COMBINATION FOR CRACK STABILITY ANALYSES

In accordance with Standard Review Plan 3.6.3 (Reference 3-1), the absolute sum of loading components can be applied which results in higher magnitude of combined loads. If crack stability is demonstrated using these loads, the LBB margin on loads can be reduced from  $\sqrt{2}$  to 1.0. The absolute summation of loads are shown in the following equations:

$$F = |F_{DW}| + |F_{TH}| + |F_P| + |F_{SSE\ INERTIA}| + |F_{SSE\ SAM}| \quad (3-7)$$

$$M_X = |(M_X)_{DW}| + |(M_X)_{TH}| + |(M_X)_{SSE\ INERTIA}| + |(M_X)_{SSE\ SAM}| \quad (3-8)$$

$$M_Y = |(M_Y)_{DW}| + |(M_Y)_{TH}| + |(M_Y)_{SSE\ INERTIA}| + |(M_Y)_{SSE\ SAM}| \quad (3-9)$$

$$M_Z = |(M_Z)_{DW}| + |(M_Z)_{TH}| + |(M_Z)_{SSE\ INERTIA}| + |(M_Z)_{SSE\ SAM}| \quad (3-10)$$

where subscripts SSE INERTIA and SSE SAM mean Safe Shutdown Earthquake Inertia and Safe Shutdown Earthquake Seismic Anchor Motion, respectively.

The loads so determined are used in the fracture mechanics evaluations (Section 7.0) to demonstrate the LBB margins at the locations established to be the governing locations. The loads at all the locations of interest (see Figure 3-2) are given in Table 3-2.

Table 3-2 shows the enveloped loads from both the loops and Table 3-1 shows the corresponding normal loads.

### 3.5 REFERENCES

- 3-1 Standard Review Plan: Public Comments Solicited; 3.6.3 Leak-Before-Break Evaluation Procedures; Federal Register/Vol. 52, No. 167/Friday, August 28, 1987/Notices, pp. 32626-32633.

<b>Location*</b>	<b>Outside Diameter (in)</b>	<b>Minimum Thickness (in)</b>	<b>Axial Load** (lbs)</b>	<b>Moment (in-lbs)</b>	<b>Total Stress (psi)</b>
1	33.875	2.333	1503000	14021826	14720
2	33.875	2.333	1503000	4671201	9240
3	33.875	2.333	1503000	4537361	9162
4	37.188	2.989	1630058	8728777	8507
5	37.188	2.989	1697988	1389966	5834
6	36.188	2.489	1694718	1545528	7176
7	36.188	2.489	1690558	1761887	7264
8	36.188	2.489	1700888	1212286	7039
9	36.188	2.489	1700888	2700010	7755
10	37.188	2.989	1760128	5262643	7550
11	32.125	2.208	1347627	3980436	9235
12	32.125	2.208	1347627	4773674	9780
13	33.063	2.676	1351747	6178548	8728

\* See Figure 3-2

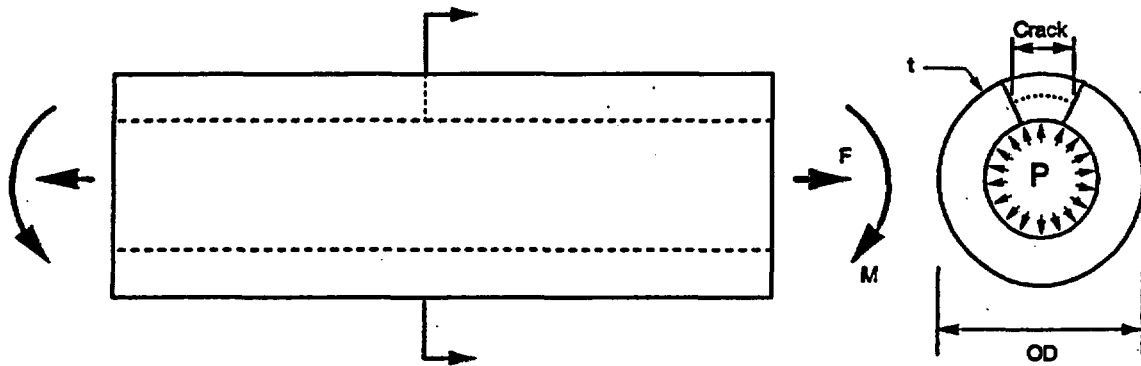
\*\* Included Pressure

<b>Table 3-2 Faulted Loads and Stresses for Ginna Station</b>			
<b>Location***</b>	<b>Axial Load*** (lbs)</b>	<b>Moment (In-lbs)</b>	<b>Total Stress (psi)</b>
1	1753880	16298576	17139
2	1753870	5255054	10668
3	1756940	6610840	11475
4	1960878	13101928	11257
5	1852998	16724794	12345
6	1789808	10914559	12045
7	1785918	4938304	9154
8	1890568	7685554	10873
9	1878728	9524594	11713
10	1803438	14004621	11121
11	1498687	11962249	15456
12	1502957	9259743	13616
13	1485327	12229487	12618

\* See Figure 3-2

\*\* See Table 3-1 for Dimensions

\*\*\* Included Pressure



$$\begin{aligned} \text{OD} &= 33.875 \text{ in} \\ t &= 2.333 \text{ in} \end{aligned}$$

Normal Loads<sup>\*</sup>

Force<sup>\*\*\*</sup>: 1503 kips  
 Moment: 14022 in-kips

Faulted Loads<sup>\*\*</sup>

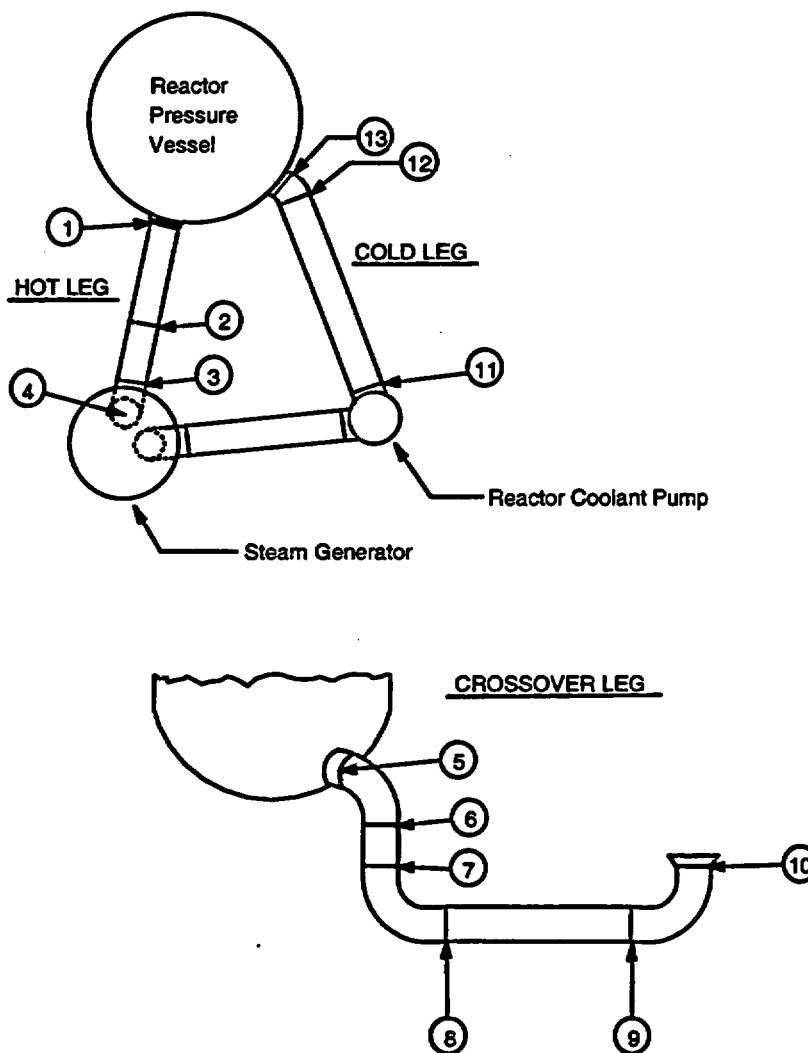
Force<sup>\*\*\*</sup>: 1754 kips  
 Moment: 16299 in-kips

<sup>\*</sup> See Table 3-1

<sup>\*\*</sup> See Table 3-2

<sup>\*\*\*</sup> Included the force due to a pressure of 2250 psia

**Figure 3-1 Hot Leg Coolant Pipe**

HOT LEG

Temperature: 603.9°F

Pressure: 2250 psia

CROSS-OVER LEG

Temperature: 543.1°F

Pressure: 2250 psia

COLD LEG

Temperature: 543.1°F

Pressure: 2250 psia

**Figure 3-2 Schematic Diagram of Ginna Station Primary Loop Showing Weld Locations**

## 4.0 MATERIAL CHARACTERIZATION

### 4.1 PRIMARY LOOP PIPE AND FITTINGS MATERIALS

The material type for the Ginna Station primary loop piping is A376 TP316 and for the elbow fittings is A351 CF8M.

### 4.2 TENSILE PROPERTIES

The piping Certified Materials Test Reports (CMTRs) for the Ginna Station were used to establish the tensile properties for the Leak-Before-Break analysis. The CMTRs include tensile properties at room temperature and/or at 650°F for each of the heats of material. These properties are given in Table 4-1 for piping and in Table 4-2 for elbows fittings.

For the A376 TP316 material, the representative properties at 603.9°F were established from the tensile properties at 650°F given in Table 4-1 by utilizing Section II of the 2001 ASME Boiler and Pressure Vessel Code (Reference 4-1). Code tensile properties at 603.9°F were obtained by interpolating between the 600°F and 650°F tensile properties. Ratios of the code tensile properties at 603.9°F to the corresponding tensile properties at 650°F were then applied to the 650°F tensile properties given in Table 4-1 to obtain the plant specific properties for A376 TP316 at 603.9°F.

The Elbow Fittings Certified Materials Test Reports (CMTRs) for the Ginna Station were used to establish the tensile properties for the Leak-Before-Break analysis. The CMTRs for elbow fittings include tensile properties at room temperature and/or at 650°F for each of the heats of material. These properties are given in Table 4-2.

For the A351 CF8M material, the representative properties at 603.9°F and 543.1°F were established from the tensile properties at 650°F given in Table 4-2 by utilizing section II of the 2001 ASME boiler and pressure vessel code. Code tensile properties at 603.9°F and 543.1°F were established by interpolating between the 500°F, 600°F and the 650°F tensile properties. Ratios of the code tensile properties at 603.9°F and 543.1°F to the corresponding properties at 650°F were then applied to the 650°F tensile properties given in Table 4-2 to obtain the plant specific representative properties for A351 CF8M at 603.9°F and 543.1°F.

The average and lower bound yield strengths and lower bound ultimate strengths are given in Table 4-3. The ASME code Moduli of Elasticity are also given in Table 4-3, and Poisson's Ratio was taken as 0.3.

### 4.3 FRACTURE TOUGHNESS PROPERTIES

The pre-service fracture toughnesses of cast stainless steels in terms of  $J_{Ic}$  have been found to be very high at 600°F. [

<sup>a,c,e</sup> However, cast stainless steel is susceptible to thermal aging at the reactor operating temperature, that is, about 290°C (550°F). Thermal aging of cast stainless steel results in embrittlement, that is, a decrease in the ductility, impact strength, and fracture toughness of the material. Depending on the material composition, the Charpy impact energy of a cast stainless steel component could decrease to a small fraction of its original value after exposure to reactor temperatures during service.

The susceptibility of the material to thermal aging increases with increasing ferrite contents. The molybdenum bearing CF8M shows increased susceptibility to thermal aging. The method described below was used to calculate the end of life toughness properties for the cast material.

In 1994, the Argonne National Laboratory (ANL) completed an extensive research program in assessing the extent of thermal aging of cast stainless steel materials. The ANL research program measured mechanical properties of cast stainless steel materials after they have been heated in controlled ovens for long periods of time. ANL compiled a database, both from data within ANL and from international sources, of about 85 compositions of cast stainless steel exposed to a temperature range of 290-400°C (550-750°F) for up to 58,000 hours (6.5 years). From this database, ANL developed correlations for estimating the extent of thermal aging of cast stainless steel (References 4-3 and 4-4).

ANL developed the fracture toughness estimation procedures by correlating data in the database conservatively. After developing the correlations, ANL validated the estimation procedures by comparing the estimated fracture toughness with the measured value for several cast stainless steel plant components removed from actual plant service. The ANL procedures produced conservative estimates that were about 30 to 50 percent less than actual measured values. The procedure developed by ANL in Reference 4-4 was used to calculate the end of life fracture toughness values for this analysis. ANL research program was sponsored and the procedure was accepted (Reference 4-5) by the NRC.

The chemical compositions are available from CMTRs and are provided in Table 4-4.

$Cr_{(eq)}$  = Chromium Equivalent

$Ni_{(eq)}$  = Nickel Equivalent

where  $Cr_{(eq)}$  and  $Ni_{eq}$  are in percent weight

$\delta_c$  = Ferrite In Percent Volume

$Cr_{(eq)}$ ,  $Ni_{(eq)}$  and  $\delta_c$  values obtained from Reference 4-2 are shown in Table 4-4.

The following equations are taken from Reference 4-4.

For CF8M steel with <10% Ni, the saturation value of saturation room temperature (RT) impact energy  $C_{Vsat}$  (J/cm<sup>2</sup>) is the lower value determined from

$$\log_{10}C_{Vsat} = 1.10 + 2.12 \exp (-0.041\phi) \quad (4-1)$$

where the material parameter  $\phi$  is expressed as

$$\phi = \delta_c (Ni + Si + Mn)^2 (C + 0.4N)/5; \quad (4-2)$$

and from

$$\log_{10}C_{Vsat} = 7.28 - 0.011\delta_c - 0.185Cr - 0.369Mo - 0.451Si - 0.007Ni - 4.71(C + 0.4N) \quad (4-3)$$

For CF8M steel with >10% Ni, the saturation value of RT impact energy  $C_{Vsat}$  (J/cm<sup>2</sup>) is the lower value determined from

$$\log_{10}C_{Vsat} = 1.10 + 2.64 \exp (-0.064\phi) \quad (4-4)$$

where the material parameter  $\phi$  is expressed as

$$\phi = \delta_c (Ni + Si + Mn)^2 (C + 0.4N)/5 \quad (4-5)$$

and from

$$\log_{10}C_{Vsat} = 7.28 - 0.011\delta_c - 0.185Cr - 0.369Mo - 0.451Si - 0.007Ni - 4.71(C + 0.4N) \quad (4-6)$$

The RT impact energies of the cast stainless steel materials were determined from the chemical compositions available from CMTRs and provided in Table 4-4.

The saturation J-R curve at 290°C(554°F) for static-cast CF8M steel is given by:

$$J_d = 49 (C_{Vsat})^{0.41} (\Delta a)^n \quad (4-7)$$

$$n = 0.23 + 0.06 \log_{10} (C_{Vsat}) \quad (4-8)$$

where  $J_d$  is the "deformation J" in kJ/m<sup>2</sup> and  $\Delta a$  is the crack extension in mm.

[

] a.c.e

[

 $J^{a,c,e}$ 

[

 $J^{a,c,e}$ 

The correlations presented in Reference 4-4 are applicable to cast stainless steels used in the U.S. nuclear industry, the steels contain <25% ferrite in almost all cases. [

 $J^{a,c,e}$ 

The results from the ANL Research Program indicate that the lower-bound fracture toughness of thermally aged cast stainless steel is similar to that of Submerged Arc Welds (SAWs). The applied value of the J-integral for a flaw in the weld regions will be lower than that in the base metal because the yield strength for the weld materials is much higher at the temperature<sup>1</sup>. Therefore, weld regions are less limiting than the cast material.

In the fracture mechanics analyses that follow, the fracture toughness properties given in Table 4-5 will be used as the criteria against which the applied fracture toughness values will be compared.

---

<sup>1</sup> In the report, all the applied J values were conservatively determined by using base metal strength properties.

---

#### 4.4 REFERENCES

- 4-1 Boiler and Pressure Vessel Code Section II, Part D – Material Properties, 2001 Edition, July 1, 2001, ASME Boiler and Pressure Vessel Committee, Subcommittee on Materials.
- 4-2 A800/A800M-84 – Standard Practice for Steel Casting, Austenitic Alloy, Estimating Ferrite Content Thereof, Section 1 – Iron and Steel Products, Vol. 01.02, Ferrous Castings; Ferroalloys; Shipbuilding.
- 4-3 O. K. Chopra and W. J. Shack, "Assessment of Thermal Embrittlement of Cast Stainless Steels," NUREG/CR-6177, U. S. Nuclear Regulatory Commission, Washington, DC, May 1994.
- 4-4 O. K. Chopra, "Estimation of Fracture Toughness of Cast Stainless Steels During Thermal Aging in LWR Systems," NUREG-CR-4513, Revision 1, U. S. Nuclear Regulatory Commission, Washington, DC, August 1994.
- 4-5 "Flaw Evaluation of Thermally aged Cast Stainless Steel in Light-Water Reactor Applications," Lee, S.; Kuo, P. T.; Wichman, K.; Chopra, O.; Published in International Journal of Pressure Vessel and Piping, June 1997.

<b>Table 4-1 Measured Tensile Properties (psi) for the Ginna Station Primary Loop Piping (Material A376 TP316)</b>						
<b>HEAT NO.</b>	<b>SERIAL NO.</b>	<b>LOCATION</b>	<b>At Room Temperature</b>		<b>At 650°F</b>	
			<b>YIELD STRENGTH (psi)</b>	<b>ULTIMATE STRENGTH (psi)</b>	<b>YIELD STRENGTH (psi)</b>	<b>ULTIMATE STRENGTH (psi)</b>
D8650	1476	Hot Leg	34500	75300	21000	65100
D8650	1476	Hot Leg	36000	76500		
D8650	1477	Hot Leg	36500	76500		
D8650	1477	Hot Leg	38000	78500		
D8632	1480	Hot Leg	36500	76200	22700	64200
D8632	1480	Hot Leg	37200	78100		
D6886	1481	Hot Leg	38000	79100	21100	65700
D6886	1481	Hot Leg	39000	80400		
D8548	1157A	Cross-over Leg	33000	75900	20800	63100
D8548	1157A	Cross-over Leg	40300	77900		
V0246	1996	Cross-over Leg	30000	75800	20600	59700
V0246	1996	Cross-over Leg	30500	75000		
D8552	1154	Cross-over Leg	37000	80400	23500	66700
D8552	1154	Cross-over Leg	40000	81400		
V0249	1982	Cross-over Leg	31400	75800	21900	63400
V0249	1982	Cross-over Leg	33000	76600		
D8647	1471	Cold Leg	36200	75200	21100	66200
D8647	1471	Cold Leg	38500	79000		
D8651	1473	Cold Leg	37000	75600	22100	60600
D8651	1473	Cold Leg	40000	80600		

**Table 4-2 Measured Tensile Properties (psi) for the Ginna Station Primary Loop Elbow Fittings (Material A351 CF8M)**

HEAT NO.	LOCATION	At Room Temperature		At 650°F	
		YIELD STRENGTH (psi)	ULTIMATE STRENGTH (psi)	YIELD STRENGTH (psi)	ULTIMATE STRENGTH (psi)
5175-1	Hot Leg	42000	90000		
01547-1	Hot Leg	49500	91000		
5038-1	Cross-over Leg	58500	98000		
00024-1	Cross-over Leg	41400	81500	25500	66750
2786-1	Cross-over Leg	54000	94500		
03182-1	Cross-over Leg	40500	84500	27000	69800
4693	Cross-over Leg	43500	87000		
4312	Cross-over Leg	55500	94000		
01493-1	Cross-over Leg	46500	91000		
01799-1B	Cross-over Leg	48000	90000		
4672	Cross-over Leg	49500	90000		
4858	Cross-over Leg	48000	88000		
2506-2	Cold Leg	52500	93500		
3764-5	Cold Leg	48000	87000		

a,c,e



a,c,e

\*Heats for the Hot Leg;  
\*\*Heats for the Cold Leg

All other heats are in cross-over leg.  
N is assumed as 0.05

<sup>1</sup>From Equations 4-1 or 4-4

<sup>2</sup>From Equations 4-3 or 4-6

<sup>3</sup>Minimum of  $C_{V_{sat}}^1$  and  $C_{V_{sat}}^2$

a,c,e



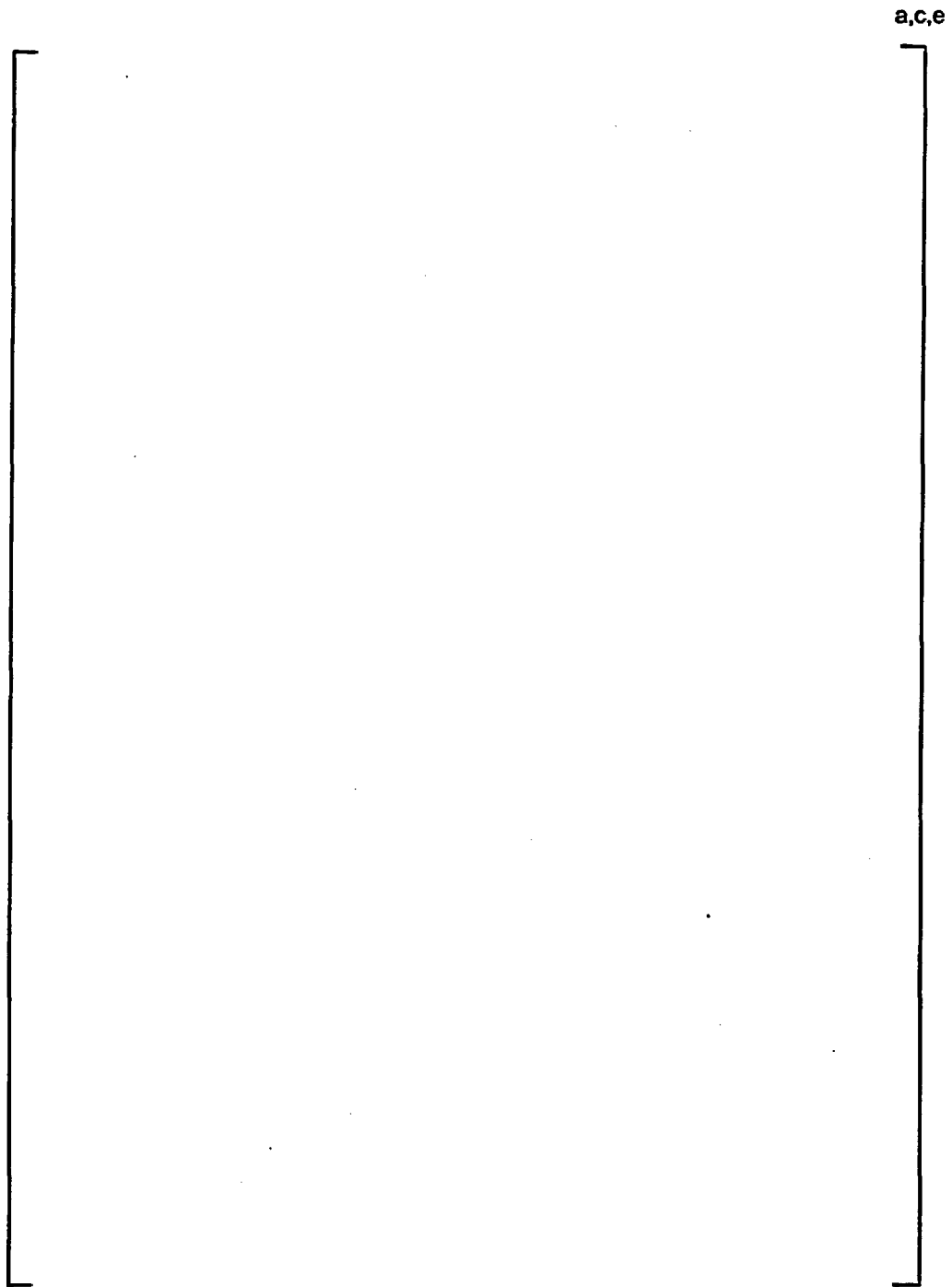


**Figure 4-1 Pre-Service J vs.  $\Delta a$  for SA351 CF8M Cast Stainless Steel at 600°F**

## 5.0 CRITICAL LOCATIONS AND EVALUATION CRITERIA

### 5.1 CRITICAL LOCATIONS

The Leak-Before-Break (LBB) evaluation margins are to be demonstrated for the limiting locations (governing locations). Candidate locations are designated as load critical location or toughness critical locations as discussed in Section 3.0. Such locations are established based on the loads in Section 3.0 and the material properties established in Section 4.0. These locations are defined below for the Ginna Station. Table 3-2 as well as Figure 3-2 are used for this evaluation.

#### Load Critical Locations

The highest stressed location for the entire primary loop is at Location 1 (in the Hot Leg) (See Figure 3-2) at the reactor vessel outlet nozzle to pipe weld. Location 1 is the critical location for all the weld locations in the primary loop piping. Since it is on a straight pipe with forged material, it is a high toughness location.

#### Toughness Critical Locations

Low toughness locations are at the ends of every elbow. In the case of the hot leg, low toughness is found for Heat No. 01547-1 (see Figure 3-2 for locations). Location 3 has the higher faulted stress than location 4 and will yield a higher  $J_{app}$ . In the case of cross-over leg and cold leg, the low toughness is found for Heat No. 4312. Location 12 has the highest faulted stress in the cross-over leg and cold leg elbow and will yield the highest  $J_{app}$ . It is thus concluded that the enveloping locations are 1, 3 and 12. The allowable toughness values for the critical locations are shown in Table 4-5.

### 5.2 FRACTURE CRITERIA

As will be discussed later, fracture mechanics analyses are made based on loads and postulated flaw sizes related to leakage. The stability criteria against which the calculated  $J$  and tearing modulus are compared are:

- (1) If  $J_{app} < J_{IC}$ , then the crack will not initiate;
- (2) If  $J_{app} \geq J_{IC}$ , but, if  $T_{app} < T_{mat}$  and  $J_{app} < J_{max}$ , then the crack is stable.

where:

$J_{app}$  = Applied  $J$

$J_{IC}$  =  $J$  at Crack Initiation

$T_{app}$  = Applied Tearing Modulus

$T_{mat}$  = Material Tearing Modulus

$J_{max}$  = Maximum J value of the material

For critical locations, the limit load method discussed in Section 7.0 was also used.

## 6.0 LEAK RATE PREDICTIONS

### 6.1 INTRODUCTION

The purpose of this section is to discuss the method, which is used to predict the flow through postulated through-wall cracks and present the leak rate calculation results for through-wall circumferential cracks.

### 6.2 GENERAL CONSIDERATIONS

The flow of hot pressurized water through an opening to a lower back pressure causes flashing which can result in choking. For long channels where the ratio of the channel length,  $L$ , to hydraulic diameter,  $D_H$ , ( $L/D_H$ ) is greater than [

] <sup>a,c,e</sup>.

### 6.3 CALCULATION METHOD

The basic method used in the leak rate calculations is the method developed by [

] <sup>a,c,e</sup>

The flow rate through a crack was calculated in the following manner. Figure 6-1 from Reference 6-1 was used to estimate the critical pressure,  $P_c$ , for the primary loop enthalpy condition and an assumed flow. Once  $P_c$  was found for a given mass flow, the [ <sup>a,c,e</sup> ] was found from Figure 6-2 (taken from Reference 6-1). For all cases considered, since [ <sup>a,c,e</sup> ] Therefore, this method will yield the two-phase pressure drop due to momentum effects ( $\Delta P_{2\phi}$ ) as illustrated in Figure 6-3, where  $P_o$  is the operating pressure. Now using the assumed flow rate,  $G$ , the frictional pressure drop can be calculated using

$$\Delta P_f = [ \quad ]^{a,c,e} \quad (6-1)$$

where the friction factor  $f$  is determined using the [ <sup>a,c,e</sup> ] The crack relative roughness,  $\epsilon$ , was obtained from fatigue crack data on stainless steel samples. The relative roughness value used in these calculations was [ <sup>a,c,e</sup> ]

The frictional pressure drop using equation 6-1 is then calculated for the assumed flow rate and added to the [ <sup>a,c,e</sup> ] to obtain the total pressure drop from the primary system to the atmosphere. That is, for the primary loop,

$$\text{Absolute Pressure} - 14.7 = [ \quad ]^{a,c,e} \quad (6-2)$$

for a given assumed flow rate G. If the right-hand side of equation 6-2 does not agree with the pressure difference between the primary loop and the atmosphere, then the procedure is repeated until Equation 6-2 is satisfied to within an acceptable tolerance which in turn leads to correct flow rate value for a given crack size.

#### 6.4 LEAK RATE CALCULATIONS

Leak rate calculations were made as a function of crack length at the governing locations previously identified in Section 5.1. The normal operating loads of Table 3-1 were applied in these calculations. The crack opening areas were estimated using the method of Reference 6-2 and the leak rates were calculated using the two-phase flow formulation described above. The average material properties of Section 4.0 (see Table 4-3) were used for these calculations.

The Ginna Station RCS pressure boundary leak detection system of 0.25 gpm meets the intent of Reg. Guide 1.45, which is 1 gpm in 1 hour or less. Thus, to satisfy the margin of 10 on the leak rate, the flaw sizes (leakage flaw sizes) are determined which yield a leak rate of 2.5 gpm.

The flaw sizes to yield a leak rate of 2.5 gpm were calculated at the governing locations and are given in Table 6-1. The flaw sizes so determined are called leakage flaw sizes.

#### 6.5 REFERENCES

6-1. [

] <sup>a,c,e</sup>.

6-2. Tada, H., "The Effects of Shell Corrections on Stress Intensity Factors and the Crack Opening Area of Circumferential and a Longitudinal Through-Crack in a Pipe," Section II-1, NUREG/CR-3464, September 1983.

a,c,e

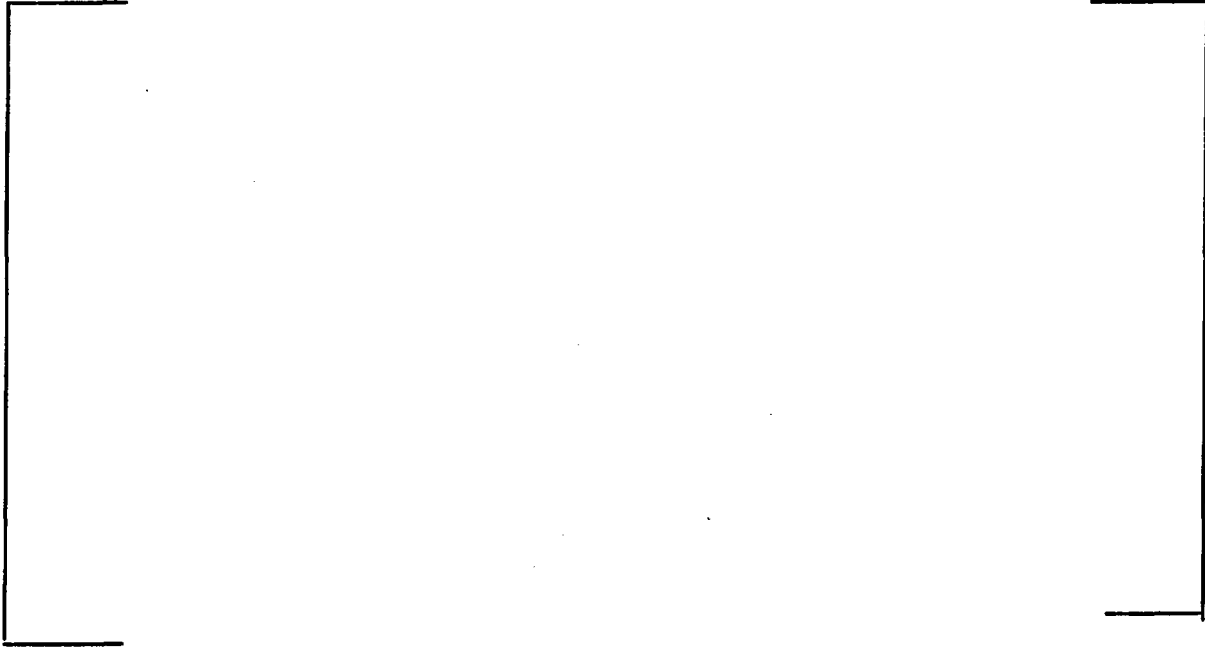




**Figure 6-1 Analytical Predictions of Critical Rates of Steam-Water Mixtures**



Figure 6-2 [

] <sup>a,c,e</sup> Pressure Ratio as a Function of  $L/D$

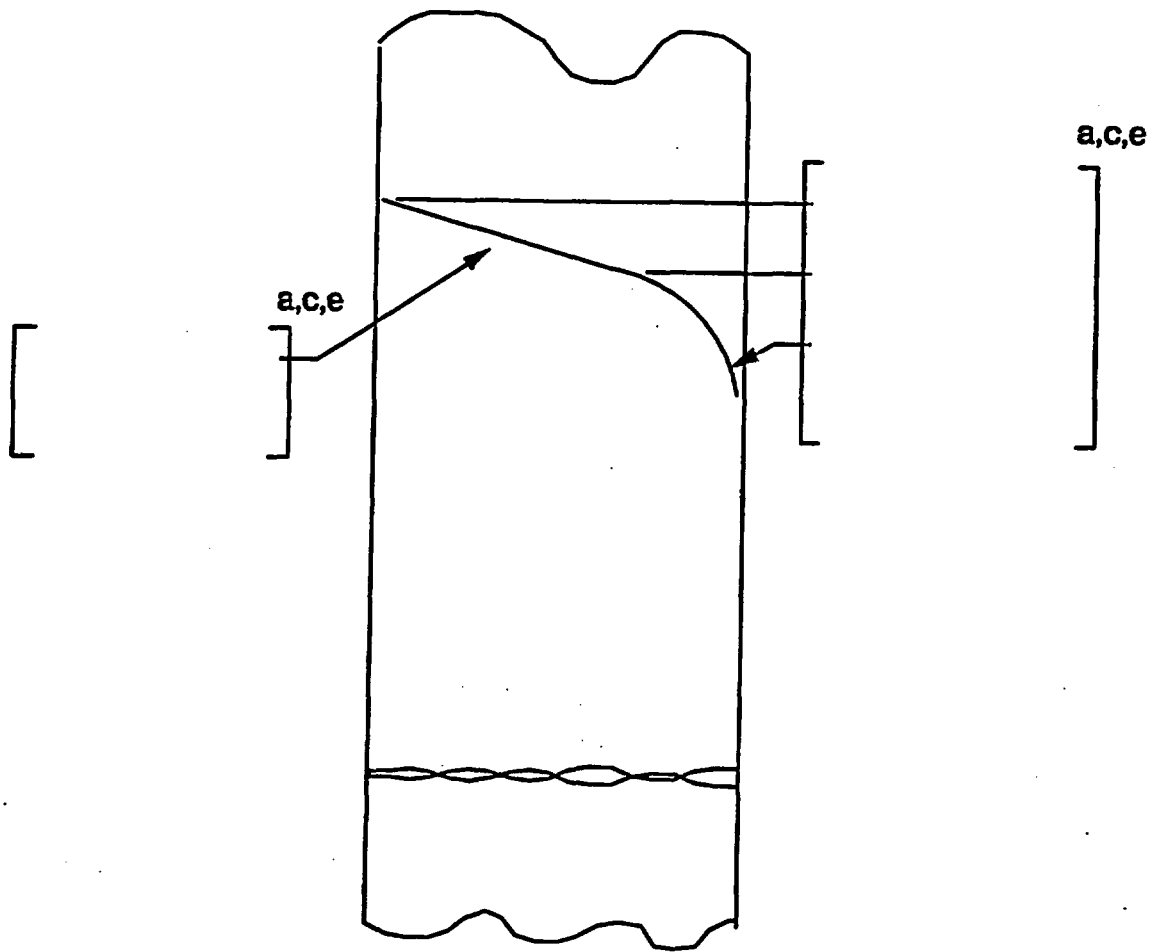


**Figure 6-3 Idealized Pressure Drop Profile Through a Postulated Crack**

## 7.0 FRACTURE MECHANICS EVALUATION

### 7.1 LOCAL FAILURE MECHANISM

The local mechanism of failure is primarily dominated by the crack tip behavior in terms of crack-tip blunting, initiation, extension and finally crack instability. The local stability will be assumed if the crack does not initiate at all. It has been accepted that the initiation toughness measured in terms of  $J_{IC}$  from a J-integral resistance curve is a material parameter defining the crack initiation. If, for a given load, the calculated J-integral value is shown to be less than the  $J_{IC}$  of the material, then the crack will not initiate. If the initiation criterion is not met, one can calculate the tearing modulus as defined by the following relation:

$$T_{app} = \frac{dJ}{da} \frac{E}{\sigma_f^2}$$

where:

$T_{app}$	=	Applied Tearing Modulus
$E$	=	Modulus of Elasticity
$\sigma_f$	=	$0.5 (\sigma_y + \sigma_u)$ = Flow Stress
$a$	=	Crack Length
$\sigma_y, \sigma_u$	=	Yield and Ultimate Strength of the Material, respectively

Stability is said to exist when ductile tearing occurs if  $T_{app}$  is less than  $T_{mat}$ , the experimentally determined tearing modulus. Since a constant  $T_{mat}$  is assumed, a further restriction is placed on  $J_{app}$ .  $J_{app}$  must be less than  $J_{max}$  where  $J_{max}$  is the maximum value of J for which the experimental  $T_{mat}$  is greater than  $T_{app}$  used.

As discussed in Section 5.2 the local crack stability criteria is a two-step process:

(1) If  $J_{app} < J_{IC}$ , then the crack will not initiate.

(2) If  $J_{app} > J_{IC}$ , but, if  $T_{app} < T_{mat}$

and  $J_{app} < J_{max}$ , then the crack is stable.

### 7.2 GLOBAL FAILURE MECHANISM

Determination of the conditions which lead to failure in stainless steel should be done with plastic fracture methodology because of the large amount of deformation accompanying fracture. One method for predicting the failure of ductile material is the plastic instability

method, based on traditional plastic limit load concepts, but accounting for strain hardening and taking into account the presence of a flaw. The flawed pipe is predicted to fail when the remaining net section reaches a stress level at which a plastic hinge is formed. The stress level at which this occurs is termed as the flow stress. The flow stress is generally taken as the average of the yield and ultimate tensile strength of the material at the temperature of interest. This methodology has been shown to be applicable to ductile piping through a large number of experiments and will be used here to predict the critical flaw size in the primary coolant loop piping. The failure criterion has been obtained by requiring equilibrium of the section containing the flaw (Figure 7-1) when loads are applied. The detailed development is provided in Appendix A for a through-wall circumferential flaw in a pipe with internal pressure, axial force, and imposed bending moments. The limit moment for such a pipe is given by:

$$[ \quad ]^{a,c,e}$$

where:

$$[$$

$$]^{a,c,e}$$

$$\sigma_f = 0.5 (\sigma_y + \sigma_u) = \text{Flow Stress, psi}$$

$$[$$

$$]^{a,c,e}$$

$$[$$

$$]^{a,c,e}$$

---

The analytical model described above accurately accounts for the piping internal pressure as well as imposed axial force as they affect the limit moment. Good agreement was found between the analytical predictions and the experimental results (Reference 7-1).

For application of the limit load methodology, the material, including consideration of the configuration, must have a sufficient ductility and ductile tearing resistance to sustain the limit load.

### **7.3 RESULTS OF CRACK STABILITY EVALUATION**

#### Local Failure Mechanism

[

J<sup>a.c.e</sup>

[

] <sup>a,c,e</sup>**Global failure mechanism**

The critical locations were also identified in Section 5.1. A stability analysis based on limit load was performed for these locations as described in Section 7.2. The welds at these locations are Gas Tungsten Arc Weld (GTAW) and Manual Metallic Arc Weld (MMAW) which is similar to Shielded Metal Arc Weld (SMAW). The "Z" factor correction for GTAW is 1.0, while that for SMAW was applied (Reference 7-5) as follows:

$$Z = 1.15 [ 1.0 + 0.013(OD-4) ]$$

where OD is the outer diameter of the pipe in inches.

The Z-factors for SMAW welds were calculated for the critical locations, using the dimensions given in Table 3-1. The calculated Z factors were 1.60, 1.60 and 1.57 for locations 1, 3 and 12 respectively. The applied loads were increased by the Z factors for SMAW welds and plots of limit load versus crack length were generated as shown in Figures 7-2, 7-3 and 7-4. Table 7-2 summarizes the results of the stability analyses based on limit load. The leakage size flaws are also presented in the same Table.

#### 7.4 REFERENCES

- 7.1 Kanninen, M. F., et. al., "Mechanical Fracture Predictions for Sensitized Stainless Steel Piping with Circumferential Cracks," EPRI NP-192, September 1976.
- 7.2 Johnson, W. and Mellor, P. B., Engineering Plasticity, Van Nostrand Reinhold Company, New York, (1973), pp. 83-86.
- 7.3 Tada, H., "The Effects of Shell Corrections on Stress Intensity Factors and the Crack Opening Area of Circumferential and a Longitudinal Through-Crack in a Pipe," Section II-1, NUREG/CR-3464, September 1983.
- 7.4 Irwin, G. R., "Plastic Zone Near a Crack and Fracture Toughness," Proc. 7<sup>th</sup> Sagamore Conference, P. IV-63 (1960).
- 7.5 Standard Review Plan; Public Comment Solicited; 3.6.3 Leak-Before-Break Evaluation Procedures; Federal Register/Vol. 52, No. 167/Friday, August 28, 1987/Notices, pp. 32626-32633.

**Notes:**

\* $T_{mat}$  is not applicable since  $J_{app} < J_{Ic}$ .

$J_{app}$  values were calculated for flaw size(s) of 2 times the 2.5 gpm leakage flaw size(s). As can be seen from Table 7-1,  $J_{app}$  values are much lower than the  $J_{Ic}$  allowable values and therefore there are ample margins available for the J calculation.



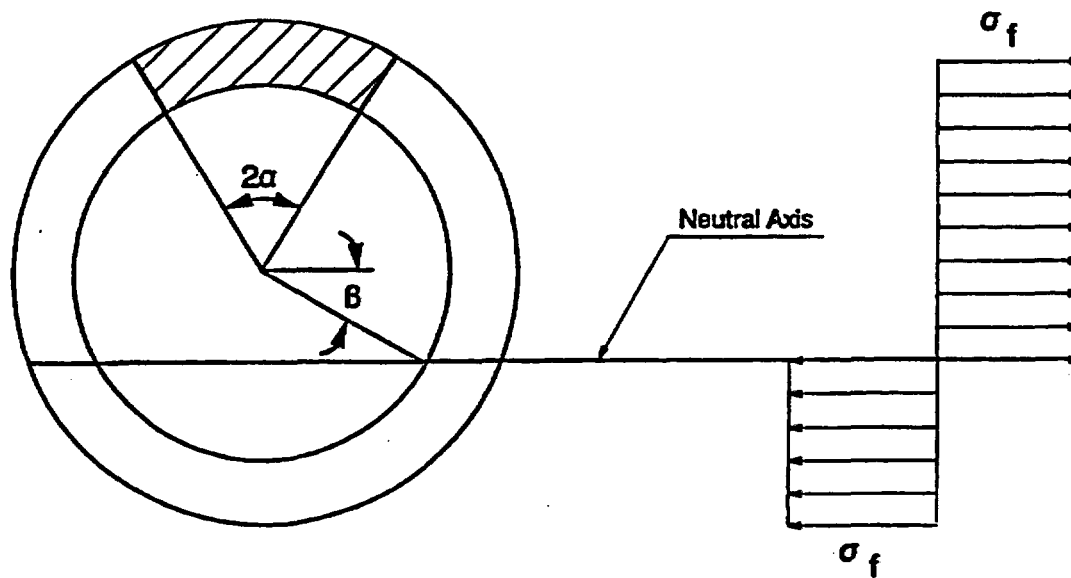


Figure 7-1 [ ]<sup>a,c,e</sup> Stress Distribution



OD = 33.875 in     $\sigma_y = 21.011$  ksi    F = 1753.88 kips  
t = 2.333 in     $\sigma_u = 59.700$  ksi    M = 16298.576 in-kips  
A376 TP316 with SMAW weld

**Figure 7-2 Critical Flaw Size Prediction – Hot Leg at Location 1**



OD = 33.875 in     $\sigma_y = 26.011$  ksi    F = 1756.94 kips  
t = 2.333 in     $\sigma_u = 66.750$  ksi    M = 6610.84 in-kips

A351 CF8M with SMAW weld

**Figure 7-3 Critical Flaw Size Prediction – Hot Leg at Location 3**



OD = 32.125 in     $\sigma_y = 26.922$  ksi    F = 1502.957 kips

t = 2.208 in     $\sigma_u = 66.750$  ksi    M = 9259.743 in-kips

A351 CF8M with SMAW weld

**Figure 7-4 Critical Flaw Size Prediction – Cold Leg at Location 12**

## 8.0 FATIGUE CRACK GROWTH ANALYSIS

To determine the sensitivity of the primary coolant system to the presence of small cracks, a fatigue crack growth analysis was carried out for the [ ]<sup>a,c,e</sup> region of a typical system (see Location [ ]<sup>a,c,e</sup> of Figure 3-2). This region was selected because crack growth calculated there would be typical of that in the entire primary loop. Crack growths calculated at other locations would be expected to show less than 10% variation.

A [ ]<sup>a,c,e</sup> of a plant typical in geometry and operational characteristics to any Westinghouse PWR system. The normal, upset, and test conditions were considered. A summary of the generic thermal transients used conservatively for the Ginna Station for 60 years is provided in Table 8-1. Circumferentially oriented surface flaws were postulated in the region. These flaws were assumed to be located in two different locations, as shown in Figure 8-1. Specifically, these were:

Cross-Section A: [ ]<sup>a,c,e</sup>

Cross-Section B: [ ]<sup>a,c,e</sup>

Fatigue crack growth rate laws were used [ ]

[ ]<sup>a,c,e</sup> The law for stainless steel was derived from Reference 8-1. A compilation of data for austenitic stainless steel in a PWR water environment was presented in Reference 8-2, and it was found that the effect of the environment on the crack growth rate was very small. From this information it was estimated that the environmental factor should be conservatively set at [ ]<sup>a,c,e</sup> in the crack growth rate equation from Reference 8-1.

For stainless steel, the fatigue crack growth formula is:

[ ]

[ ]<sup>a,c,e</sup>

The calculated fatigue crack growth for semi-elliptic surface flaws of circumferential orientation and various depths is summarized in Table 8-2. The result shows that the crack growth for 60

years is very small, [ ]<sup>a,c,e</sup> Therefore fatigue crack growth is not a concern for the Ginna Station primary loop piping.

## 8.1 REFERENCES

- 8-1 James, L. A. and Jones, D. P., "Fatigue Crack Growth Correlations for Austenitic Stainless Steel in Air, Predictive Capabilities in Environmentally Assisted Cracking," ASME publication PVP-99, December 1985.
- 8-2 Bamford, W. H., "Fatigue Crack Growth of Stainless Steel Piping in a Pressurized Water Reactor Environment," Trans. ASME Journal of Pressure Vessel Technology, Vol. 101, Feb. 1979.

<b>Table 8-1 Summary of Reactor Vessel Transients (60 Years)</b>		
<b>Number</b>	<b>Transient Identification</b>	<b>Number of Cycles</b>
	<b>Normal Conditions</b>	
1	Heatup and Cooldown at 100°F/hr	200
2	Load Follow Cycles (Unit Loading and Unloading at 5 %of full power/min)	18300
3	Step Load Increase and Decrease	2000
4	Large Step Load Decrease, with Steam Dump	200
5	Steady State Fluctuations	1x10 <sup>6</sup>
	<b>Upset Conditions</b>	
6	Loss of Load (Without immediate Turbine or Reactor Trip)	80
7	Loss of power (Blackout with natural circulation in the Reactor Coolant System)	40
8	Loss of Flow (Partial Loss of Flow, one pump only)	80
9	Reactor Trip From Full Power	400
	<b>Test Conditions</b>	
10	Turbine Roll Test	10
11	Hydrostatic Test Conditions - Primary Side Leak Test	50
12	Cold Hydrostatic Test	10

Table 8-2 Fatigue Crack Growth at [ ] <sup>a,c,e</sup> ( 60 years)		
Initial Flaw (in.)	Final Flaw (in.)	
	[ ] <sup>a,c,e</sup>	[ ] <sup>a,c,e</sup>
[ ]		
		[ ] <sup>a,c,e</sup>

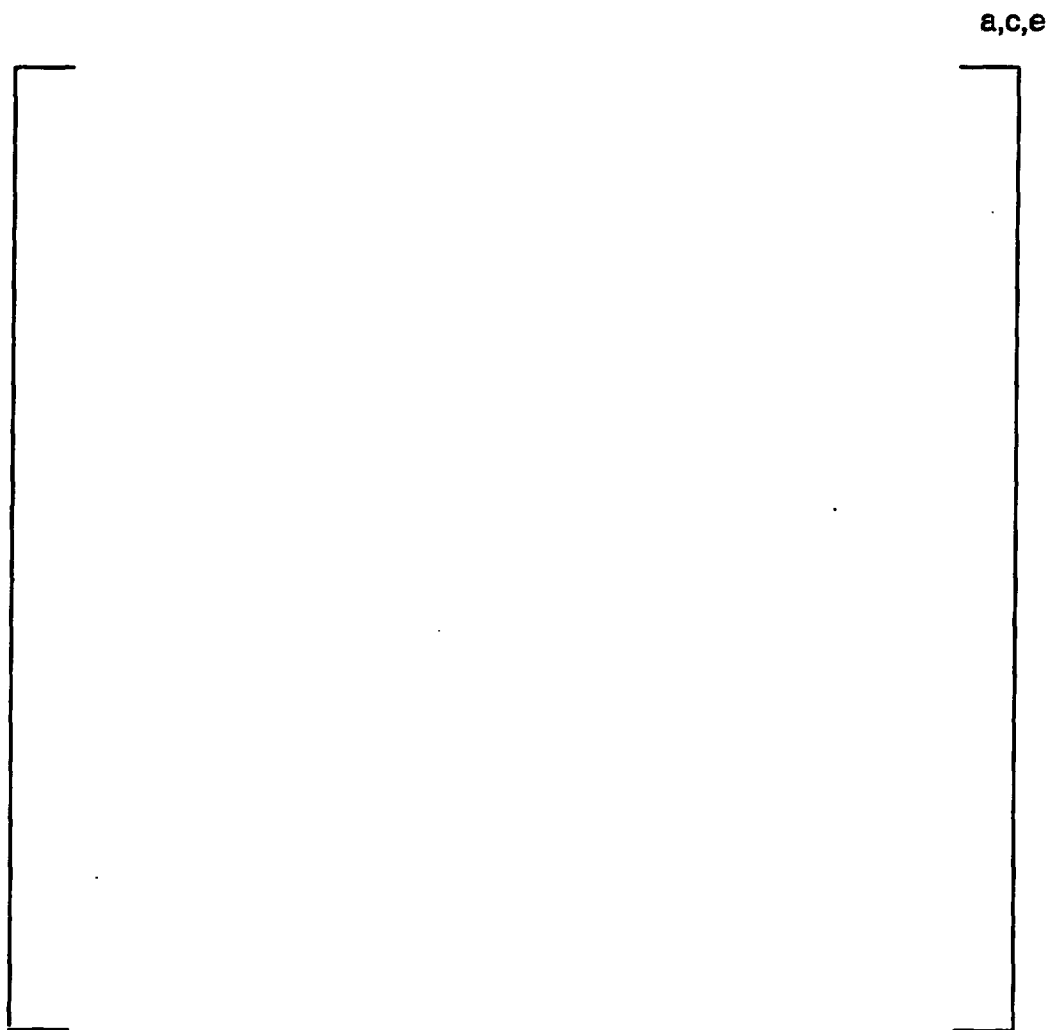
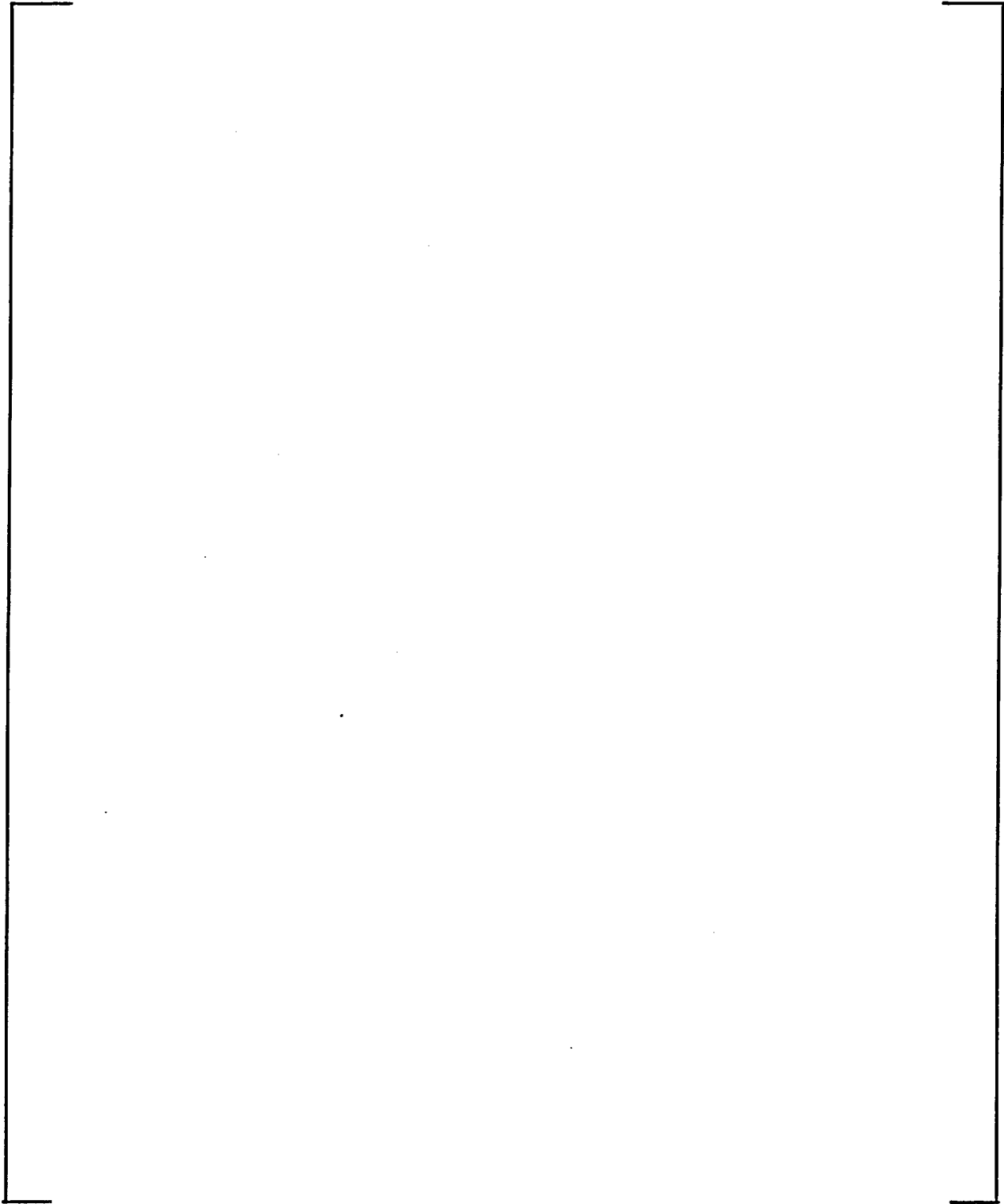


Figure 8-1 Typical Cross-Section of [ ]<sup>a,c,e</sup>



**Figure 8-2 Reference Fatigue Crack Growth Curves for Carbon and Low Alloy Ferritic Steels**

## 9.0 ASSESSMENT OF MARGINS

The results of the leak rates of Section 6.4 and the corresponding stability and fracture toughness evaluations of Sections 7.1, 7.2 and 7.3 are used in performing the assessment of margins. Margins are shown in Table 9-1.

In summary, at all the critical locations relative to:

1. Flaw Size - Using faulted loads obtained by the absolute sum method, a margin of 2 or more exists between the critical flaw and the flaw having a leak rate of 2.5 gpm (the leakage flaw).
2. Leak Rate - A margin of 10 exists between the calculated leak rate from the leakage flaw and the leak detection capability of 0.25 gpm.
3. Loads - At the critical locations, the leakage flaw was shown to be stable using the faulted loads obtained by the absolute sum method (i.e., a flaw twice the leakage flaw size is shown to be stable; hence the leakage flaw size is stable). A margin on loads  $>1$  using the absolute summation of faulted load combinations is satisfied.

a,c,e

---

\* Based on Limit Load

\*\* Based on J Integral Evaluation [Note: margin on flaw size(s) is greater than 2 since  $J_{app}$  values for critical flaw size(s) of 2 times the leakage flaw size(s) are much lower than the  $J_{IC}$  values as shown in Table 7-1]

## 10.0 CONCLUSIONS

This report justifies the elimination of RCS primary loop pipe breaks from the structural design basis for the 60 year plant life of Ginna Nuclear Power Plant as follows:

- a. Stress corrosion cracking is precluded by the use of fracture resistant materials in the piping system and controls on the reactor coolant chemistry, temperature, pressure, and flow during normal operation.
- b. Water hammer should not occur in the RCS piping because of the system design, testing, and operational considerations.
- c. The effects of low and high cycle fatigue on the integrity of the RCS piping are negligible.
- d. Ample margin exists between the leak rate of small stable flaws and the capability of the Ginna Nuclear Power Plant Reactor Coolant System Pressure Boundary Leakage Detection System.
- e. Ample margin exists between the small stable leakage flow sizes of item (d) and larger stable critical flaw sizes.
- f. Ample margin exists in the J-integral material properties used to demonstrate end-of-service life (relative to aging) stability for the critical flaws. Based on the stability analysis results, Cast Austenitic Stainless Steel (CASS) elbow material of Ginna Nuclear Power Plant primary loop piping is not an issue.

For the critical locations, flaws are identified that will be stable because of the ample margins described in items (d), (e), and (f) above.

Based on the above, the Leak-Before-Break conditions are satisfied for the Ginna Nuclear Power Plant RCS piping. All the recommended margins are satisfied. It is therefore concluded that the dynamic effects of RCS primary loop pipe breaks need not be considered in the structural design basis of the Ginna Nuclear Power Plant for the 60 year plant life as part of the License Renewal Program.

**APPENDIX A**  
**LIMIT MOMENT**

[

]a.c.e



**Figure A-1 Pipe with a Through-Wall Crack in Bending**